

Frictional impact of a rigid disk on an elastic cable

S.R. Eugster

Institute of Mechanical Systems, Center of Mechanics, ETH Zurich, CH-8092 Zürich, Switzerland

Abstract. In this paper a novel approach for the inclusion of hard contacts, i.e. perfect unilateral constraints, in a finite element framework is presented. The finite element formulation is derived for a two-dimensional representation of a cable. Higher-order element shape functions using Bézier functions allow for the introduction of contact points arbitrary in number and position along the element and enable the contact forces to follow the ongoing motion. The contact laws, which express the impenetrability in normal direction and Coulomb friction law in tangential direction, can adequately be formulated as normal cone inclusions. The developed cable element has no bending stiffness, is linear elastic and allows for large deformation. Moreau's time-stepping algorithm is used for the numerical time-integration. The novel approach is demonstrated on the example of a frictional impact of a rigid disk on an elastic cable.

Keywords: Contact, Friction, Deformable Body, Nonlinear Finite Element Method

PACS: 02.70.Dh; 45.50.Tn; 46.70.Hg

INTRODUCTION

An impact of a rigid disk on a deformable cable is a non-smooth dynamical problem where the formulation of the contact-impact problem have to conform with the formulation of the deformation of the body, i.e. the finite element formulation. In [1] generalized contact-impact laws are introduced and by using proximal point methods a time integration algorithm is presented, based on Moreau's time-stepping algorithm [2]. In order to use this time-stepping algorithm, the equations of motion have to arise in the following form

$$\mathbf{M}(\mathbf{q}) \cdot \ddot{\mathbf{q}} - \mathbf{h}(t, \mathbf{q}, \dot{\mathbf{q}}) - \sum_{i \in \mathcal{H}} \mathbf{w}_i \cdot \lambda_i = 0, \quad \gamma_i = \mathbf{w}_i^T \cdot \dot{\mathbf{q}}, \quad \gamma_i \in \mathcal{N}_{\mathcal{C}_i}(-\lambda_i), \quad (1)$$

where \mathbf{M} is the symmetric mass matrix, $\mathbf{q}(t)$ is the vector with the generalized coordinates, \mathbf{h} is the vector with all smooth elastic, gyroscopic and dissipating generalized forces and λ_i are the constraint forces of the bilateral constraints and contact forces of the normal and tangential contacts. The vectors $\mathbf{w}_i(\mathbf{q})$ are the corresponding generalized force directions which also appear in the relative constraint velocities γ_i . The force laws of the contact forces connecting γ_i with λ_i are formulated as normal cone inclusions, characterized by a given set \mathcal{C}_i . Depending on the chosen set \mathcal{C}_i one gets different normal cones representing different physical force laws. To read more about normal cone inclusions one may refer to [1]. $\mathcal{H}(\mathbf{q}, t) := \{\mathcal{S}_B \cup \mathcal{S}_N \cup \mathcal{S}_T\}$ is the set of indices of the closed contacts. Where $\mathcal{S}_B := \{Bj, j = 1, 2, \dots, n_B\}$ indicates the n_B bilateral constraints, $\mathcal{S}_N := \{Nj \mid g_{Nj}(\mathbf{q}, t) = 0, j = 1, \dots, n_{CP}\}$ and $\mathcal{S}_T := \{Tj \mid g_{Tj}(\mathbf{q}, t) = 0, j = 1, \dots, n_{CP}\}$ indicate the normal and tangential contacts, respectively. The aim of this paper is the contact formulation between a disk and a cable. The contact kinematics and the proper force laws should be formulated in the sense of Equation (1). Firstly, the problem is described in detail. Subsequently, the kinematics is introduced in which Bézier curves as element shape function are used. Lastly, the derivation of the contact formulation between disk and cable is treated.

Problem Description

The dynamical system depicted in Figure (1a) consists of a disk and a cable. The disk is considered as a rigid body and is characterized by its radius R [m] and its mass m_D [kg]. The upper end of the cable is fixed at height h [m] above the ground, the lower end is pinned such that the cable is prestressed by a constant tension T [N]. The cable has an undeformed length L [m], mass density ρ_0 [kg/m] and stiffness k [N] and has no bending stiffness. The interaction between the disk and the cable is modeled as a hard, unilateral contact in the normal direction and as a Coulomb type friction with friction coefficient μ [–] in the tangential direction. The entire system is subjected to gravitation given

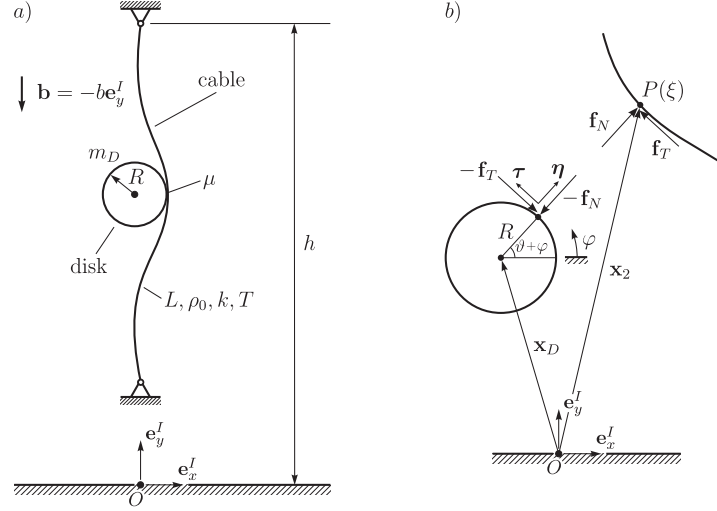


FIGURE 1. a) A sketch of the modeled system which consists of a disk and a cable. b) Free body diagram of a contact situation between a point on the cable $P(\xi)$ and the rigid disk.

by the acceleration \mathbf{b} [m/s²]. The system is modeled by its 2-dimensional representation in the xy -plane. The position space is spanned by the orthonormalized, inertial basis $(0, \mathbf{e}_x^I, \mathbf{e}_y^I)$. The acceleration \mathbf{b} has only non-zero components in the axial direction, namely $\mathbf{b} = -b\mathbf{e}_y^I$ with $b = 9.81$ [m/s²].

MECHANICAL MODELING

Kinematics

The modeled system can be seen as a material set $\mathcal{S} = \mathcal{S}_1 \cup \mathcal{S}_2$, where \mathcal{S}_1 and \mathcal{S}_2 are the collections of all material points P of the disk and the rope, respectively [3]. The motion of the two bodies is expressed by a finite number of generalized coordinates $\mathbf{q}(t) \in \mathcal{Q} \subseteq \mathbb{R}^N$, the material points $P \in \mathcal{S}$, parameterized by $(r, \vartheta) \in \bar{\Omega}_1 = [0, R] \times [0, 2\pi]$ and $\xi \in \bar{\Omega}_2 = [0, L]$, and the time $t \in \mathcal{T}$. Thus, the motion of the disk \mathbf{x}_1 as a 2-dimensional body and the cable \mathbf{x}_2 as a 1-dimensional body is seen as a map to the position space \mathcal{V}

$$\begin{aligned} \mathbf{x}_1 : \mathcal{Q} \times \bar{\Omega}_1 \times \mathcal{T} &\rightarrow \mathcal{V} & \mathbf{x}_2 : \mathcal{Q} \times \bar{\Omega}_2 \times \mathcal{T} &\rightarrow \mathcal{V} \\ (\mathbf{q}, (r, \vartheta), t) &\mapsto \mathbf{x}_1(\mathbf{q}, (r, \vartheta), t) & (\mathbf{q}, \xi, t) &\mapsto \mathbf{x}_2(\mathbf{q}, \xi, t) \end{aligned} \quad (2)$$

Since the disk is considered to be rigid, the motion of a point (r, ϑ) on the disk is defined by the position of the midpoint $\mathbf{x}_D(t) = (x(t) \ y(t))^T$ and the rotation angle $\varphi(t)$ depicted in Figure(1b) and can therefore be written as

$$\mathbf{x}_1 = \mathbf{x}_1(\mathbf{q}_1, (r, \vartheta)) = \begin{pmatrix} x(t) \\ y(t) \end{pmatrix} + r \begin{pmatrix} \cos(\varphi(t) + \vartheta) \\ \sin(\varphi(t) + \vartheta) \end{pmatrix}, \quad \mathbf{q}_1(t) = (x \ y \ \varphi)^T, \quad (3)$$

where $\mathbf{q}_1 = \mathbf{L}_1 \cdot \mathbf{q}$ are the local generalized coordinates extracted out of the global generalized coordinates \mathbf{q} using a Boolean matrix \mathbf{L}_1 , called connectivity matrix [4]. The implementation of the connectivity matrix is part of the meshing process and therefore \mathbf{L} can be considered as a known matrix.

The cable as a continuous structure, parameterized by $\bar{\Omega}_2$ with infinite many degrees of freedom has to be discretized by n_e elements. Inside the elements, the kinematics is described by spatial element shape functions

$$\begin{aligned} \mathbf{x}_2^e : \hat{\Omega}_2^e \times \mathcal{Q} &\rightarrow \mathcal{V} \\ (\xi^e, \mathbf{q}_2^e) &\mapsto \mathbf{x}_2^e(\xi^e, \mathbf{q}_2^e), \end{aligned} \quad (4)$$

where ξ^e is the element coordinate and $\mathbf{q}_2^e = \mathbf{L}_2^e \cdot \mathbf{q}$ are the local generalized coordinates. For an appropriate model of the cable the spatial element function \mathbf{x}_2^e have to be at least a polynomial of degree three. Whereas a linear polynomial

guarantees C^0 -continuity, a quadratic polynomial guarantees in addition C^1 -continuity (differentiability). But it is still possible that the direction of the curve changes in a connecting node, i.e. inversion occurs. Therefore information about the incoming and outgoing direction in a node is needed. Using cubic B ezier curves the directions are formulated by two aiming points p_2 and p_3 , cf. Figure (2b). The function

$$\mathbf{x}_2^e = \mathbf{x}_1 + (\xi^e)^2(3 - 2\xi^e)(\mathbf{x}_4 - \mathbf{x}_1) + 3\xi^e(1 - \xi^e)^2 r_1 \mathbf{e}_\varphi(\varphi_1) - 3(\xi^e)^2(1 - \xi^e) q_4 \mathbf{e}_\varphi(\varphi_4) \quad \xi^e \in [0, 1] \quad (5)$$

can be described by eight local coordinates

$$\mathbf{q}_2^e(t) = (x_1 \ y_1 \ r_1 \ \varphi_1 \ x_4 \ y_4 \ q_4 \ \varphi_4) . \quad (6)$$

and is depicted In Figure (2b) for the interval $\xi^e \in [0, 1]$. At $\xi^e = 0$, the point p_1 with the position $\bar{\mathbf{x}}_1 = (x_1 \ y_1)$ is located with a weighted gradient $r_1 \mathbf{e}_\varphi(\varphi_1)$, where $\mathbf{e}_\varphi(\varphi) = (\cos(\varphi) \ \sin(\varphi))^T$. At $\xi^e = 1$, point p_4 is located with position $\bar{\mathbf{x}}_4 = (x_4 \ y_4)$ and a weighted gradient $q_4 \mathbf{e}_\varphi(\varphi_4)$. In Figure (2a) one can see a node N_i , which is the connecting point between two elements. The angle φ_i and the position of the node x_i and y_i belong to the node and are called nodal degrees of freedom. On the contrary, the weight factors r_i and q_i are element degrees of freedom. Hence, the discretized rope with n_e elements and $n_n = n_e + 1$ nodes holds $ndof = 3n_n + 2n_e$ degrees of freedom.

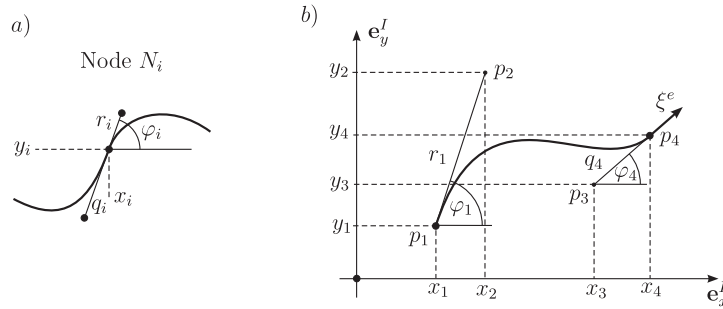


FIGURE 2. a) The position x_i, y_i and the angle φ_i belong to a node N_i . The weight factors r_i and q_i are degrees of freedom of the element. b) The element on the domain $\hat{\Omega}^e \in [0, 1]$ can be described by eight local coordinates \mathbf{q}_2^e .

Contact formulation

During the contact between disk and cable line distributed contact forces in normal and tangential direction of the contact line occur, denoted by \mathbf{l}_N and \mathbf{l}_T . The contact forces act as external forces and contribute $\int_{\mathcal{S}} d\mathbf{f}^c \cdot \delta \mathbf{x}$ to the virtual work of the system. After introducing generalized coordinates \mathbf{q} and following the principle of d'Alembert-Lagrange, the strong form of the equilibrium equations are achieved where the contact forces take the form

$$\int_{\mathcal{S}} d\mathbf{f}^c \cdot \frac{\partial \mathbf{x}}{\partial \mathbf{q}} = \int_{\partial\Omega_1} d\vartheta R(-\mathbf{l}_N - \mathbf{l}_T) \cdot \frac{\partial \mathbf{x}_1}{\partial \mathbf{q}} + \int_{\Omega_2} d\xi (\mathbf{l}_N + \mathbf{l}_T) \cdot \frac{\partial \mathbf{x}_2}{\partial \mathbf{q}} . \quad (7)$$

The contact forces interact on the contact line, i.e. between the boundary of the disk $\partial\Omega_1$ and the domain of the cable Ω_2 . In the kinematically discretized model the distributed contact forces will typically degenerate into concentrated forces at a limited number of points, the positions of which are a priori unknown. Therefore a convenient approach is to introduce a dense grid of n_{CP} possible contact points at arbitrarily given material points of the rope and approximate in the sense

$$\int_{\partial\Omega_1} d\vartheta R(-\mathbf{l}_N - \mathbf{l}_T) \cdot \frac{\partial \mathbf{x}_1}{\partial \mathbf{q}} + \int_{\Omega_2} d\xi (\mathbf{l}_N + \mathbf{l}_T) \cdot \frac{\partial \mathbf{x}_2}{\partial \mathbf{q}} \approx \sum_{j=1}^{n_{CP}} \left[(\mathbf{f}_N(\xi) + \mathbf{f}_T(\xi)) \cdot \left(\frac{\partial \mathbf{x}_2}{\partial \mathbf{q}} - \frac{\partial \mathbf{x}_1}{\partial \mathbf{q}} \right) \right]_j . \quad (8)$$

Thus, the interaction is modeled pointwise as a hard, unilateral contact in the normal direction and as a Coulomb type friction with friction coefficient μ in the tangential direction. Therefore, the constitutive law will be introduced for a general material point P on the rope with coordinate ξ which is in contact with the disk.

It is convenient to introduce a normal and tangential direction $\boldsymbol{\eta}(\xi)$ and $\boldsymbol{\tau}(\xi)$, respectively. The normal direction $\boldsymbol{\eta}$ for a contact point on the rope is the normalized connection line between the the position of the disk's midpoint \mathbf{x}_D

and the position of the contact point \mathbf{x}_2 itself. The tangential direction $\boldsymbol{\tau}$ is orthogonal to the normal direction and is introduced as depicted in Figure (1b) and is achieved by a rotation of the normal

$$\boldsymbol{\eta} = \frac{\mathbf{x}_2 - \mathbf{x}_D}{\|\mathbf{x}_2 - \mathbf{x}_D\|}, \quad \boldsymbol{\tau} = \mathbf{R}\boldsymbol{\eta}, \quad \mathbf{R} = (\mathbf{e}_x^I \otimes \mathbf{e}_y^I - \mathbf{e}_y^I \otimes \mathbf{e}_x^I). \quad (9)$$

With the introduction of normal and tangential directions $\boldsymbol{\eta}$ and $\boldsymbol{\tau}$, the contact forces can be written as $\mathbf{f}_N = \lambda_N(\xi)\boldsymbol{\eta}$ and $\mathbf{f}_T = \lambda_T(\xi)\boldsymbol{\tau}$.

After the discretization of the rope by finite elements a relation between the n_{CP} contact points on the rope, which can be chosen arbitrarily, have to be given. During the meshing process, where a grid of contact points j is generated, the connection to the element $e(j)$ and the element coordinate $\xi^{e(j)}$ is stored. Using this information Equation (8) is reformulated in the sense of Equation (1)

$$\begin{aligned} \sum_{j=1}^{n_{CP}} \left[(\mathbf{f}_N(\xi) + \mathbf{f}_T(\xi)) \cdot \left(\frac{\partial \mathbf{x}_2}{\partial \mathbf{q}} - \frac{\partial \mathbf{x}_1}{\partial \mathbf{q}} \right) \right]_j &= \sum_{j=1}^{n_{CP}} (\lambda_{Nj}\boldsymbol{\eta}^j + \lambda_{Tj}\boldsymbol{\tau}^j) \cdot \left(\frac{\partial \mathbf{x}_2^{e(j)}}{\partial \mathbf{q}_2^e} \cdot \mathbf{L}_2^{e(j)} - \frac{\partial \mathbf{x}_1}{\partial \mathbf{q}_1} \cdot \mathbf{L}_1 \right) \\ &= \sum_{j=1}^{n_{CP}} (\mathbf{w}_{Nj}\lambda_{Nj} + \mathbf{w}_{Tj}\lambda_{Tj}). \end{aligned} \quad (10)$$

CONCLUSIONS

The impact of the disk and the ongoing motion of both bodies after the impact can be simulated successfully using Moreau's time-stepping algorithm and generates reasonable results, cf. Figure (3), though benchmark examples or analytical solutions are yet missing.

The great advantage of the presented procedure is the decoupling of the number of contact points from the number of elements. To avoid, that the simulated disk flies through the cable, a dense grid of contact points is needed. Conversely, due to the high order of the shape function just a few elements are sufficient to develop the basic eigenmodes of the pinned cable. Thus, it would be numerically highly inefficient if the contact points are bound to the element nodes and the number of contact points have to coincide with the number of elements. Additionally high frequency eigenmodes which decay very fast are damped out numerically without an introduction of material damping. For future projects one can imagine adaptive contact grid refinement at the positions of contact.

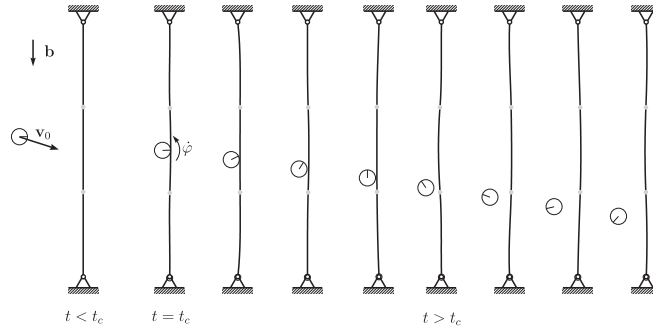


FIGURE 3. Simulation of the frictional impact with initial velocity \mathbf{v}_0 and gravity \mathbf{b} .

REFERENCES

1. Ch. Glocker, "Simulation von harten Kontakten mit Reibung: Eine iterative Projektionsmethode," in *VDI-Berichte No. 1968: Schwingungen in Antrieben 2006 Tagung, Fulda*, VDI Verlag, Düsseldorf, 2006, vol. 1968.
2. J. J. Moreau, "Unilateral Contact and Dry Friction in Finite Freedom Dynamics," in *Moreau, J. J., Panagiotopoulos, P.D. u. Strang, G. (Eds.): Non-Smooth Mechanics and Applications, CISM Courses and Lectures*, Springer Verlag, Wien, 1988, vol. 302, pp. 1–74.
3. P. Chadwick, *Continuum Mechanics, Concise Theory and Problems*, Dover Publications Inc., New York, 1976, ISBN 0-486-40180-4.
4. T. Belytschko, W. K. Liu, and B. Moran, *Nonlinear Finite Elements for Continua and Structures*, Wiley, New York, 2000.